Mineralogical Magazine, August 2011, Vol. 75(4), pp. 2467–2484

Review

Potassium-bearing clinopyroxene: a review of experimental, crystal chemical and thermodynamic data with petrological applications

O. G. Safonov[1,2], L. Bindi[3,4,*] and V. L. Vinograd[5]

[1] Institute of Experimental Mineralogy, Russian Academy of Science, Academician Ossipian str. 4, 142432, Russia
[2] Department of Geology, University of Johannesburg, Auckland Park, Johannesburg 2006, South Africa
[3] Museo di Storia Naturale, sezione di Mineralogia, Universitá degli Studi di Firenze, Via La Pira, 4, I-50121, Florence, Italy
[4] CNR – Istituto di Geoscienze e Georisorse, sezione di Firenze, Via La Pira, 4, I-50121, Florence, Italy
[5] Institute of Energy and Climate Research, Forschungszentrum Jülich GmbH 1, 52425 Jülich, Germany

[*Received 18 March 2011; Accepted 15 June 2011*]

ABSTRACT

Available experimental data on chemical composition and crystal structure of K-bearing clinopyroxenes are compiled together with the results of atomistic simulations and thermodynamic calculations of mineral equilibria. It is shown that the limited solubility of K_2O in clinopyroxene from crustal rocks cannot be ascribed to the strong non-ideality of mixing between diopside ($CaMgSi_2O_6$) and K-jadeite ($KAlSi_2O_6$) components. The more likely reason is the instability of the potassic endmember with respect to other K-bearing phases. As the volume effects of typical K-jadeite-forming reactions are negative, the incorporation of K in the clinopyroxene structure becomes less difficult at higher pressure. Atomistic simulations predict that the thermodynamic mixing properties of diopside–K-jadeite solid-solutions at high temperature approach those of a regular mixture with a relatively small positive excess enthalpy. The standard enthalpy of formation ($\Delta_f H^0 = -2932.7$ kJ/mol), the standard volume ($V^0 = 6.479$ J mol^{-1} bar^{-1}) and the isothermal bulk modulus ($K_0 = 145$ GPa) of K-jadeite were calculated from first principles, and the standard entropy ($S^0 = 141.24$ J mol^{-1} K^{-1}) and thermal-expansion coefficient ($\alpha = 3.3 \times 10^{-5}$ K^{-1}) of the K-jadeite endmember were estimated using quasi-harmonic lattice-dynamic calculations based on a force-field model. The estimated thermodynamic data are used to compute compositions of K-bearing clinopyroxenes in diverse mineral assemblages within a wide *P-T* interval. The review substantiates the conclusion that clinopyroxene can serve as an effective container for K at upper-mantle conditions.

Keywords: clinopyroxene, mantle rocks, igneous geochemistry, igneous mineralogy, potassium.

Introduction

Understanding the content and distribution of K_2O in the mantle is important for three reasons. First, the radioactive decay of the ^{40}K isotope contributes significantly to the internal heat budget of the Earth. Second, potassium stabilizes hydrous phases (e.g. phlogopite), and thus fixes water content in some parts of the upper mantle (e.g. Konzett and Ulmer, 1999; Konzett and Fei, 2000). Third, potassium is an incompatible element that strongly partitions into the melts and fluids released during partial melting and de-volatilization of mantle peridotites and subducted crustal material (e.g. Schmidt, 1996; Thomsen and Schmidt, 2008). Being added to mantle

* E-mail: luca.bindi@unifi.it
DOI: 10.1180/minmag.2011.075.4.2467

peridotites and eclogites via fluids, potassium causes appreciable decrease of their solidus temperatures and favours the formation of potassium-rich magmas (e.g. Spandler *et al*., 2008; Foley *et al*., 2009). The estimated K_2O content of the pyrolite primitive mantle is ~0.03 wt.% (Jagoutz *et al.*, 1979; Hart and Zindler, 1986; McDonough and Sun, 1995). However, certain geochemical data imply the existence of hidden reservoirs of potassium, which could substantially increase this value (e.g. McDonough *et al.*, 1992).

The mobility of potassium at mantle conditions poses the problem of estimation of K_2O activity in mineral-forming media, and thus the host phases for potassium. Among a wide range of potassium-rich crystalline phases that are potentially stable at mantle conditions (Harlow and Davies, 2004), only sanidine, phlogopite and K-bearing amphibole occur in typical mantle assemblages. The formation of these phases depends largely on water and silica activities, and thus their sole occurrence in mineral assemblages cannot serve as the principal sensor for potassium activity. Here, we argue that the K-content of clinopyroxene is an ideal choice for such an indicator. Indeed, clinopyroxene occurs widely in both peridotitic and eclogitic mantle assemblages. It can coexist both with silicate and carbonate-silicate melts, and fluids of diverse composition. Its modal abundance and composition change regularly with *P-T* conditions and is generally insensitive to water and silica activities. Among other mantle minerals, only garnet has similar properties. However, experimental data show that measurable amounts of potassium can be incorporated into garnet only at pressures above 20 GPa (e.g. Wang and Takahashi, 1999). At upper-mantle conditions, the principal anhydrous host for potassium is clinopyroxene as supported by numerous observations. Early studies of diamondiferous eclogites and inclusions in diamonds from South African and Yakutian kimberlites noted clinopyroxene with high K_2O contents (Erlank and Kushiro, 1970; Sobolev, 1977; Prinz *et al*., 1975; Bishop *et al*., 1978). Few authors (e.g. Erlank and Kushiro, 1970) attributed high K_2O concentrations in clinopyroxenes to micro-inclusions of amphibole. Other researchers (Sobolev, 1977; Bishop *et al*., 1978) considered that potassium admixture is a specific feature of clinopyroxenes from the deep parts of the mantle and should be interpreted as isomorphic substitution. Referring to the experiments of Shimizu (1971), who succeeded in synthesizing clinopyroxene with 0.22 wt.% of K_2O at 10 GPa, Sobolev (1977) predicted that the potassium content of clinopyroxene (KCpx) should increase at upper-mantle pressures. Nevertheless, strong scepticism in relation to clinopyroxene as a carrier of potassium existed during the 1980s (e.g. Mellini and Cundari, 1989). Papike (1980) stated that "...the only major element that can not be accommodated in the pyroxene structure is K...".

This situation changed at the end of the 1980s when Ricard *et al*. (1989) and Jaques *et al*. (1990) described clinopyroxene from inclusions in diamond and peridotitic xenoliths in kimberlite and lamproite containing up to 1.5 wt.% of K_2O. Sobolev and Shatsky (1990) described similar clinopyroxene in garnet-clinopyroxene-carbonate rocks of the Kokchetav high-pressure complex. During the last 20 years, these observations were repeatedly supported by new findings of K-rich clinopyroxene inclusions in kimberlitic diamond (Sobolev *et al*., 1998; Stachel *et al*., 2000; Kaminsky *et al*., 2000; Pokhilenko *et al*., 2004). The microprobe, TEM and single-crystal X-ray diffraction study of clinopyroxene inclusions in diamond from African kimberlites by Harlow and Veblen (1991) gave conclusive evidence that clinopyroxene contains potassium in solid solution. Harlow and Veblen (1991) were the first to propose that potassium-bearing clinopyroxene is not only an indicator of high-pressure conditions, but also is a signature of "unusually K-rich environments". Numerous experimental data on KCpx coexisting with K-rich silicate melts in diverse natural and synthetic silicate systems (Edgar and Vukadinovic, 1993; Mitchell, 1995; Edgar and Mitchell, 1997; Luth, 1992, 1995, 1997; Tsuruta and Takahashi, 1998; Wang and Takahashi, 1999; Harlow, 1999, 2002; Safonov *et al*., 2003, 2004, 2005*a*) support this conclusion. Clinopyroxenes with 3.00 to 5.75 wt.% K_2O were synthesized at 7–10 GPa in K-rich carbonate-silicate and alumino-silicate systems (Harlow, 1997, 1999; Matveev *et al*., 2000; Chudinovskikh *et al*., 2001; Safonov *et al*., 2002, 2003, 2004, 2006). These experiments proved that higher pressures favour higher K_2O contents in clinopyroxene and that the potassium enrichment of clinopyroxene reflects the composition of the crystallization medium (see reviews by Perchuk *et al*., 2002; Safonov *et al*., 2005*b*). These experiments implied that clinopyroxenes can contain much higher concentrations of potassium than

those typically found in inclusions in diamonds. The findings of natural clinopyroxene with 1.97 wt.% (Plá Cid *et al*., 2003), 2.34 wt.% (Ghorbani and Middlemost, 2000) and 3.61 wt.% (Bindi *et al*., 2003) K_2O support this conclusion.

The experiments on KCpx synthesis in model systems led to an understanding of the general factors governing the potassium content in clinopyroxene (Perchuk *et al*., 2002; Safonov *et al*., 2005*b*). Experimental studies of the system $CaMgSi_2O_6$–$NaAlSi_2O_6$–$KAlSi_2O_6$ (Safonov *et al*., 2003, 2004), the unit-cell parameters of synthetic samples (Bindi *et al*., 2002, 2006) and the atomistic modelling study of Vinograd *et al*. (2010) allowed characterization of the crystal-chemical and thermodynamic properties of KCpx solid-solution. The purpose of the present paper is to give a coherent account of these results and to emphasize the view that clinopyroxene is likely to be the main host for potassium in the upper mantle.

Experimental data on K-bearing endmembers in clinopyroxene

Figure 1 shows that K content of synthetic KCpx increases with pressure up to ~7–8 GPa in all studied assemblages. In some assemblages, however, it levels off or even decreases at higher pressures. Moreover, the limiting solubility varies greatly from system to system. These variations are determined by variations in the temperature, pressure, potassium, alumina and silica activities of the coexisting melts, and by the clinopyroxene crystal chemistry (Perchuk *et al*., 2002; Safonov *et al*., 2005*b*). It is interesting to note that the same limiting content at 7–10 GPa of ~25 mol.% of $KAlSi_2O_6$ is observed in chemically diverse systems (Safonov *et al*., 2003; Chudinovskikh *et al*., 2001; Harlow, 1997). The specific feature of these systems is their oversaturation in K_2O, which is expressed in the formation of potassium silicate (SWd) (for a list of abbreviations used, see the Appendix). The phase diagram constructed on the basis of the systematic experiments at 7 GPa in the pseudo-binary join $CaMgSi_2O_6$–$KAlSi_2O_6$ (Safonov *et al*., 2003) shows that endmember K-jadeite is unstable with respect to the ternary assemblage Ks + SWd + Ky (Liu, 1987). Figure 2 shows that the KJd content of clinopyroxene increases with decrease in temperature and reaches a maximum at the solidus. The maximum solubility of KJd in clinopyroxene is determined by its equilibrium with garnet and Si-wadeite (dashed line at 75 mol.% of $KAlSi_2O_6$ in Fig. 2):

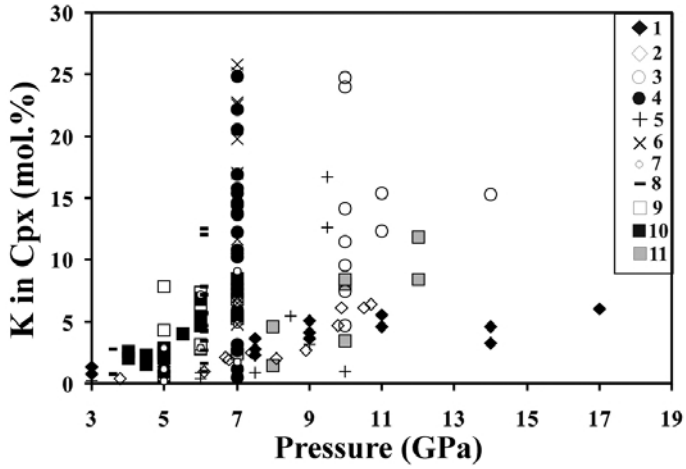

FIG. 1. Compilation of the data on K content in clinopyroxene produced in various sets of experiments. Model systems: (1) diopside–phlogopite (Luth, 1997); (2) diopside–F-phlogopite (Harlow, 2002); (3) various Cpx–K-rich carbonate systems (Harlow, 1997); (4) pyrope–grossular–K_2CO_3 (Chudinovskikh *et al*., 2001; Safonov *et al*., 2002); (5) diopside(±jadeite)–sanidine (Harlow, 1999); (6) diopside–leucite (Safonov *et al*., 2003); (7) diopside–jadeite–leucite (Safonov *et al*., 2004); (8) diopside–sanidine (Safonov *et al*., 2005*a*). Experiments on melting of natural rocks: (9) melting of K-rich lamproite (Edgar and Vukadinovic, 1993); (10) melting of sanidine-phlogopite lamproite (Mitchell, 1995); (11) melting of SiO_2-rich lamproite (Edgar and Mitchell, 1997).

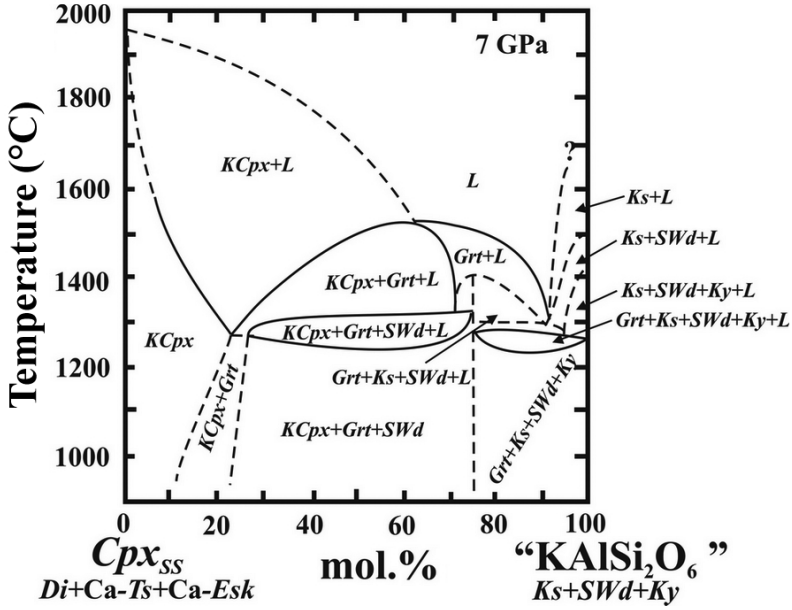

FIG. 2. Phase diagram for the pseudo-binary system $CaMgSi_2O_6$–$KAlSi_2O_6$ at 7 GPa (modified after Safonov *et al.*, 2003). Solid lines denote experimentally constrained phase boundaries whereas dashed lines show the phase boundaries which are not experimentally constrained. In the subsolidus, pure $KAlSi_2O_6$ decomposes to *Ks* + *SWd* + *Ky* (Liu, 1987).

$$4KJd + 3Di \rightleftharpoons Grs + Prp + 2SWd \qquad (1a)$$

This multi-variant reaction truncates the right branch of the 'solvus' of the KCpx solid solution and gives rise to the assemblage KCpx + Grt + SWd. The limiting concentration of K-jadeite in clinopyroxene is 23−25 mol.%. This value is close to the concentration of KJd in KCpx synthesized by Chudinovskikh *et al.* (2001) in the system pyrope-grossular-K_2CO_3 at the same pressure. The experimental products obtained by Chudinovskikh *et al.* (2001) contained the association of KCpx with pyrope-grossular garnet and Si-wadeite. This suggests that the limiting solubility of KJd in clinopyroxene is controlled by reaction 1*a*. The association of Si-wadeite and KCpx was also observed by Harlow (1997) in the systems $CaMgSi_2O_6$–$NaAlSi_2O_6$–K_2CO_3 and $CaMgSi_2O_6$–$NaCrSi_2O_6$–K_2CO_3 at 10−11 GPa. In the latter system, KCpx with a maximum K content of 22 mol.% of $KCrSi_2O_6$ coexisted with SWd and eskolaite (Cr_2O_3). This implied that the decomposition of the $KCrSi_2O_6$ (K-kosmochlor) component is governed by the reaction:

$$2KKo = SWd + Cr_2O_3 \qquad (1b)$$

Si-wadeite and garnet, the products of the KCpx decomposition, were also observed in the experiments in the ternary system $CaMgSi_2O_6$–$NaAlSi_2O_6$–$KAlSi_2O_6$ at 6 and 7 GPa (Safonov *et al.*, 2004). However, the limiting concentration of the KJd endmember in Cpx in the ternary system seemed much lower than in the binary system $CaMgSi_2O_6$–$KAlSi_2O_6$. The compositions of clinopyroxene in the experiments of Safonov *et al.* (2004) showed a negative correlation between K and Na contents (Fig. 3). A similar correlation was observed in inclusions of K-bearing omphacites in diamonds (e.g. Sobolev *et al.*, 1998; Kaminsky *et al.*, 2000; Pokhilenko *et al.*, 2004). Safonov *et al.* (2004) have argued that this effect provides a constraint on the mixing properties of diopside–K-jadeite solid-solution. Indeed, the substitution mechanism of both diopside–K-jadeite and diopside–jadeite solid-solutions can be described by the schemes $^{M1}Mg + {}^{M2}Ca \rightleftharpoons {}^{M1}Al + {}^{M2}K$ and $^{M1}Mg + {}^{M2}Ca \rightleftharpoons {}^{M1}Al + {}^{M2}Na$. An alternative description is possible in terms of the reciprocal reactions:

$$[CaMg]Si_2O_6 + [KAl]Si_2O_6 \rightarrow \{[CaAl]Si_2O_6\}^+ + \{[KMg]Si_2O_6\}^- \qquad (2)$$

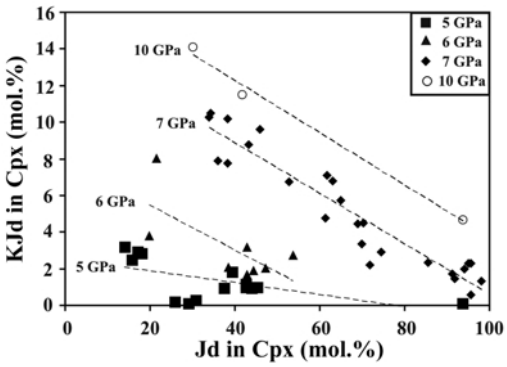

FIG. 3. Limiting effect of jadeite on K-jadeite content in K-Na-Ca clinopyroxene at 5, 6, 7 and 10 GPa (Safonov *et al*., 2004). Data at 10 GPa are taken from Harlow (1997). Dashed lines are drawn as least-squares approximations of the experimental data at each pressure.

and

$$[CaMg]Si_2O_6 + [NaAl]Si_2O_6 \rightarrow \{[CaAl]Si_2O_6\}^+ + \{[NaMg]Si_2O_6\}^- \quad (3)$$

The observed positive correlation of K at M2 with Al at M1 and the negative correlation of K with Mg at M1 for clinopyroxene in the system $CaMgSi_2O_6$–$KAlSi_2O_6$ (Fig. 4; Safonov *et al*., 2003) indicate that reaction 2 is shifted to the left and thus $\Delta G_{(2)} > 0$ (Wood and Nichols, 1979). The analogous reaction 3, which is relevant for diopside–jadeite solid solution, is also strongly displaced to the left, so that $\Delta G_{(3)} > 0$ (Wood and Nichols, 1978; Wood *et al*., 1980). Combination of reactions 2 and 3 gives the exchange equilibrium:

$$[NaAl]Si_2O_6 + \{[KMg]Si_2O_6\}^- \rightleftharpoons [KAl]Si_2O_6 + \{[NaMg]Si_2O_6\}^- \quad (4)$$

Safonov *et al*. (2004) have argued that the positive correlation of ^{M2}K with ^{M1}Mg and the negative correlation of ^{M2}K with ^{M1}Al observed in clinopyroxenes of the system $CaMgSi_2O_6$–$NaAlSi_2O_6$–$KAlSi_2O_6$ at 7 GPa (Fig. 4*b*) indicate that reaction (4) is also shifted to the left, and $\Delta G_{(4)} > 0$. The combination of all the observations suggests that $\Delta G_{(3)} > \Delta G_{(2)} > 0$. As magnitudes of the energy effects of reciprocal reactions determine degrees of non-ideality in multi-site solid solutions (Wood and Nichols, 1978), Safonov *et al*. (2004) concluded that Di-KJd solid solution should be less non-ideal than the

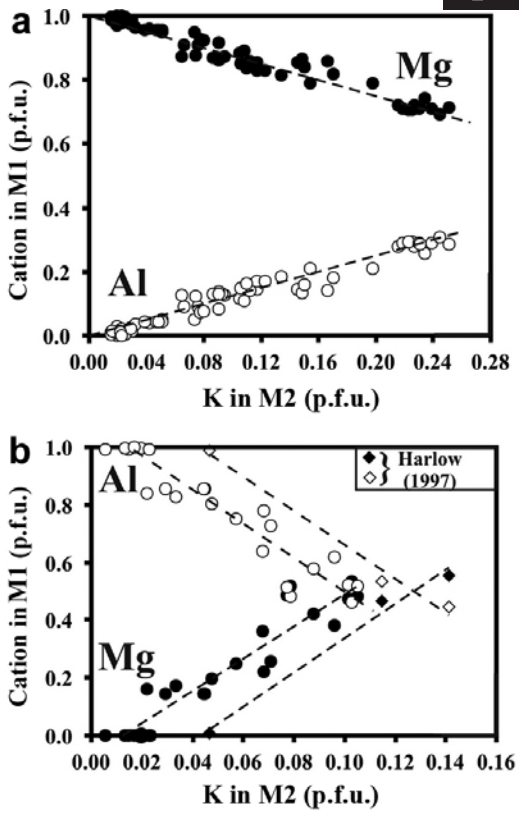

FIG. 4. Correlations of K in synthetic clinopyroxene with cations at the M1 site. (*a*) Positive correlation of ^{M2}K with ^{M1}Al (dashed lines with white dots) and negative correlation of ^{M2}K with ^{M1}Al (dashed lines with black dots) in KCpx in the system $CaMgSi_2O_6$–$KAlSi_2O_6$ at 7 GPa (Safonov *et al*., 2003). (*b*) Opposite correlations of ^{M2}K with ^{M1}Al and ^{M1}Mg (dashed lines with white and black dots, respectively) in clinopyroxene synthesized at 7 GPa in the system $CaMgSi_2O_6$–$NaAlSi_2O_6$–$KAlSi_2O_6$ (Safonov *et al*., 2004).

Di–Jd solid solution. As the diopside-jadeite solid solution shows complete mixing within the disordered *C*2/*c* phase above ~900ºC (e.g. Carpenter, 1980; Vinograd, 2002), similar behaviour is expected for the diopside-K-jadeite solid solution. However, the principal difference between these solid solutions is that in the diopside–jadeite system, the endmember $NaAlSi_2O_6$ is stable, while in the diopside–K-jadeite system, the endmember $KAlSi_2O_6$ is unstable. In this respect, a close topological analogue of the diopside–K-jadeite solid-solution is the enstatite–Mg-Tschermak solid-solution at

ambient pressure (Arima and Onuma, 1977), where the endmember $MgAl_2SiO_6$ breaks down to the assemblage enstatite solid-solution + cordierite + forsterite via the reaction

$$2En + \tfrac{2}{3}Mg\text{-}Ts \rightarrow Fo + \tfrac{1}{3}Crd \quad (5)$$

so that compositions above ~10 mol.% of Mg-Ts are unstable.

Thus, the available experimental data and the qualitative analysis based on the reciprocal-solution model suggest that the limited solubility of the K-bearing endmember in the clinopyroxene solid-solution is not related to the non-ideality of this solid solution. On the contrary, the experiments clearly show that the decomposition of the potassic endmembers of the clinopyroxene solid-solution is related to their instability with respect to other K-bearing phases (e.g. Si-wadeite). Thus, the cause of the instability of the KCpx solid-solution should be related to the thermodynamic properties of the potassic clinopyroxene endmembers and to specific crystal-chemical effects caused by the incorporation of cations which are not fully compatible with the clinopyroxene structure.

Crystal-chemical effects of potassic endmembers on the KCpx solid-solution

Structural modifications caused by K at ambient pressure

Crystal-chemical effects caused by the incorporation of diverse cations into the clinopyroxene structure are most clearly seen by comparing the structures of pure endmembers. The coupled substitution leads to simultaneous changes in size and shape of the *M*2, *M*1 and *T* polyhedra. Even where the occupancy of the M1 site is fixed, the average *M*1−O distance changes in response to the occupancy of the M2 site. Benna *et al.* (1987) have shown that the incorporation of Sr (1.26 Å) instead of Ca (1.12 Å) (data on ionic radii with eight-fold coordination are taken from Shannon, 1976) at the M2 site of diopside causes an increase of *M*1−O bond lengths and a slight expansion of the tetrahedra (Fig. 5*a*,*b*). Thus, incorporation of cations larger than Ca into M2 causes expansion of the clinopyroxene structure (TREND-1 in Fig. 5*a*). In contrast, the incorporation of Al (0.535 Å) or Cr^{3+} (0.615 Å) instead of Mg at the M1 site results in contraction of both *M*1 and *M*2 polyhedra. This effect is important for the diopside–jadeite (Wood *et al.*, 1980) (TREND-2 in Fig. 5*a*), diopside–kosmochlor (Ikeda and Yagi, 1972), diopside–Ca-Tschermak (Newton *et al.*, 1977) (TREND-3 in Fig. 5*a*), and diopside–Ca-Eskola (Wood and Henderson, 1978) solid-solutions. In the diopside-jadeite and diopside–kosmochlor solid-solutions, both Al and Cr in M1 are smaller than Mg, respectively, whereas Na is just slightly larger than Ca at M2. Thus, the substitutions at both M1 and M2 cause an overall decrease of cation–oxygen distances and of the unit-cell volume.

According to Harlow (1996) and Bindi *et al.* (2002), K occurs at the eight-coordinated M2 site. Consistent with the TREND-1 (Fig. 5*a*), the incorporation of K inevitably results in expansion of both *M*2 and *M*1 polyhedra. Incorporation of a trivalent cation (Al^{3+}, Cr^{3+}, Fe^{3+}) at the M1 site causes contraction of the clinopyroxene structure. Thus substitution of KM^{3+} (where *M* = Al, Cr, Fe^{3+}) results in competition between the expansion and the contraction effects, and has a dramatic effect on the cation–anion distances of

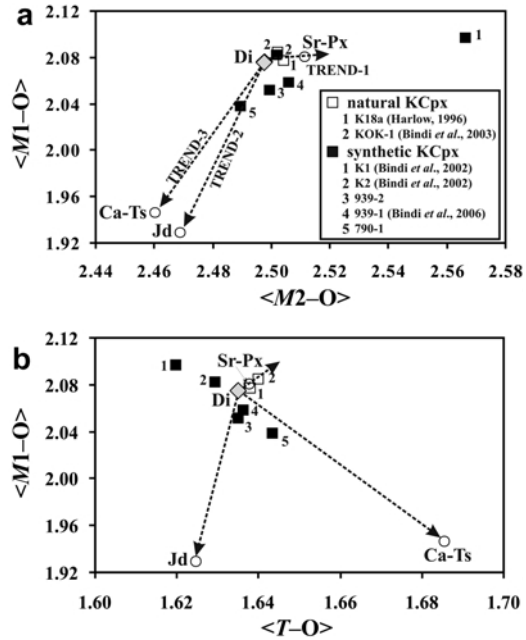

FIG. 5. Joint modifications of the average interatomic distances in the *M*1 and *M*2 polyhedra (*a*) and *M*1 and *T* polyhedra (*b*) of synthetic and natural KCpxs with respect to values for diopside. Bond distances are given in Å. Dashed arrows indicate general tendencies in changing of the interatomic distances via formation of solid solutions of diopside with $SrMgSi_2O_6$ (Benna *et al.*, 1987) (TREND-1), jadeite (Wood *et al.*, 1980) (TREND-2) and Ca-Tschermak molecule (Newton *et al.*, 1977) (TREND-3).

the *M*1 polyhedron. Harlow (1996) reported a refinement of a KCpx inclusion (from an African diamond) containing 1.57 wt.% of K_2O (K18a in Harlow and Veblen, 1991; Table 1). He noted that K causes expansion of the *M*2 polyhedron, whereas its effect on the M1 site is rather small. Harlow (1996) attributed the latter observation to the incorporation of Mg and Na at M2 that counterbalances the effect of K. He suggested that small cations such as Mg and Na at the M2 site serve to stabilize K in clinopyroxene by providing a balance of distortions of different signs. The sample K18a contains Cr, which also contributes to the general balance of distortions around the M1 site. Similar tendencies are seen in clinopyroxene from the Kokchetav Complex containing 3.61 wt.% K_2O (sample KOK-1, Bindi *et al*., 2003; Table 1). The substitution of K causes only a slight increase in *M*2–O distances. This small effect can be explained by the presence of Mg and Fe^{2+} at the M2 site (Bindi *et al*., 2003). The weak expansion of the *M*1 octahedron can be attributed to the presence of 20 mol.% Ca-Tschermak component in KOK-1. However, the T site of KOK-1 expands much less than would be expected for Ca-Ts-rich pyroxene with a similar amount of Ca-Ts (Okamura *et al*., 1974). The effect can be attributed to the influence of K. An increase in the *M*2–O distances results in shortening of the *T*–O distances (Bindi *et al*., 2003).

Thus detailed structural investigations of clinopyroxenes K18a and KOK-1 allow identification of the main structural changes due to K at M2. However, the presence of extra cations does not allow evaluation of the 'pure effect' of KM^{3+} substitution on the clinopyroxene structure. Synthetic samples offer a possibility for further investigation. The KCpx crystals synthesized in the join $CaMgSi_2O_6$–$KAlSi_2O_6$ at 7 GPa (Safonov *et al*., 2003) contain low concentrations of additional endmembers (Ca-Ts, Ca-Esk; Table 1) and thus reflect structural modifications caused by pure $^{M1}Mg + {}^{M2}Ca \rightleftharpoons {}^{M1}Al + {}^{M2}K$ substitution (Bindi *et al*., 2002). The strongest effects were observed in the crystal with 5 wt.% K_2O (or 23 mol.% KJd, K1 in Bindi *et al*., 2002; Table 1). The expansion of the *M*2 polyhedron is clearly accompanied by expansion of the *M*1 octahedron with only a slight contraction of the *T* tetrahedron (Fig. 5*a* and *b*) and an increase in cell volume. A similar coherent expansion of the *M*2 and *M*1 polyhedra was measured in sample K2 which contains 7.2 mol.% KJd (Bindi *et al*., 2002; Table 1). Both the crystals follow the TREND-1 (Fig. 5*a*).

The samples 939-1 and 939-2, containing 11.9 and 10.0 mol.% KJd, respectively (Table 1), show a different trend, where the *M*1 octahedron contracts while the *M*2 polyhedron expands slightly (Fig. 5*a*). This trend resembles that of the Di-Jd substitution. Thus, it seems that the jadeite-type mechanism of structural change (TREND-2 in Fig. 5*a*) dominates at moderately high KJd content. However, further increase in the KJd content causes a transition to TREND-1 behaviour (Fig. 5*a*). As the KJd content approaches 23 mol.% (e.g. the sample K1), the unit-cell volume increases suddenly. This increase in the cell-volume may define the stability limit of KCpx solid-solution. The catastrophic opposite effects of K and Al in clinopyroxene on the M1 site finally lead to the breakdown of *M*1–O bonds. The Al cation tends to occupy the smaller octahedron provided by garnet, while K cation prefers the larger nine-coordinated site in the Si-wadeite structure (Swanson and Prewitt, 1983). This could serve as a crystal-chemical explanation for decomposition of Di–KJd solid-solution with formation of the Grt + SWd assemblage via reaction (1*a*).

Sample 790-1 (Table 1), which along with 11 mol.% of KJd contains 25 mol.% Ca-Ts, allows comparison of structural modifications caused by simultaneous solution of both components in clinopyroxene. The presence of Ca-Ts in clinopyroxene 790-1 determines its structural distinction from pure diopside, i.e. decrease of <*M*1–O> and <*M*2–O> (TREND-3 in Fig. 5*a*) and increase of <*T*–O> (Fig. 5*b*). Despite a relatively high KJd content, the unit-cell volume of this clinopyroxene is only 432.01 $Å^3$. The unit-cell volumes of samples 939-1 and 939-2 with close KJd contents (Table 1) are notably larger. Thus, the incorporation of additional 'low-volume' components (such as Ca-Ts) in KCpx with <15 mol.% of KJd prevents the clinopyroxene structure from the rapid expansion that seems to stabilize KCpx. A similar stabilizing effect of clinoenstatite component on KCpx was discussed by Harlow (1996, 1997). However, the stabilizing effects of Ca-Ts or CEn endmembers does not mean that they assist enrichment of potassium in clinopyroxene. On the contrary, Harlow (1997) and Safonov *et al*. (2005*a*) pointed to a negative influence of these components on the solubility of K-bearing endmembers in clinopyroxene solid-solutions.

TABLE 1. Chemical analyses (wt.%) and crystal-chemical characteristics of synthetic and natural K-rich clinopyroxenes considered in the text.

Crystal sample	K1[(1)]	K2[(1)]	939-1[(2)]	939-2	790-1	KOK-1[(3)]	K18a[(4)]
SiO_2	54.55	53.71	54.85	55.44	48.42	43.92	54.30
TiO_2	0.00	0.00	0.00	0.00	0.00	0.03	0.01
Al_2O_3	7.08	4.95	4.46	2.59	14.32	23.15	0.68
Cr_2O_3	0.00	0.00	0.00	0.00	0.00	0.02	2.44
Fe_2O_3	0.00	0.00	0.00	0.00	0.00	n.d.	0.17
FeO	0.00	0.00	0.00	0.00	0.00	4.12	1.76
MgO	13.93	16.51	15.42	16.55	11.87	7.84	17.50
MnO	0.00	0.00	0.00	0.00	0.00	0.29	0.08
CaO	19.46	23.21	22.75	23.28	22.98	15.66	20.30
Na_2O	0.00	0.00	0.00	0.00	0.00	0.66	0.33
K_2O	5.00	1.57	2.60	2.17	2.39	3.61	1.57
Total	100.02	99.95	100.08	100.03	99.98	99.30	99.10
Crystal-chemical formulae on the basis of six oxygen atoms							
T site							
Si	1.967	1.934	1.976	1.999	1.750	1.608	1.992
Al	0.033	0.066	0.024	0.001	0.250	0.392	0.008
M1 site							
Mg	0.732	0.856	0.835	0.891	0.640	0.392	0.880
Fe^{2+}	0.000	0.000	0.000	0.000	0.000	0.000	0.024
Ti	0.000	0.000	0.000	0.000	0.000	0.001	0.000
Cr	0.000	0.000	0.000	0.000	0.000	0.001	0.070
Al	0.268	0.144	0.165	0.109	0.360	0.607	0.021
M2 site							
Ca	0.752	0.895	0.878	0.899	0.890	0.614	0.798
Fe^{2+}	0.000	0.000	0.000	0.000	0.000	0.126	0.036
Mg	0.016	0.030	0.000	0.000	0.000	0.036	0.070
Mn	0.000	0.000	0.000	0.000	0.000	0.009	0.000
Na	0.000	0.000	0.000	0.000	0.000	0.047	0.023
K	0.230	0.072	0.119	0.100	0.110	0.169	0.073
Vacancies	0.002	0.003	0.003	0.001	0.000	0.000	0.000
Proportions of endmembers in solid solution (mol.%)							
Di	71.6	82.6	85.0	89.6	64.0	22.2	81.0
Hed	0.0	0.0	0.0	0.0	0.0	0.0	0.0
Jd	0.0	0.0	0.0	0.0	0.0	4.5	0.0
Ca-Ts	3.3	6.6	2.4	0.1	25.0	39.2	0.8
Ca-Esk	0.5	0.6	0.6	0.3	0.0	0.0	0.0
KJd + KKo*	23.0	7.2	11.9	10.0	11.0	16.9	7.3
CEn	1.6	3.0	0.0	0.0	0.0	3.6	7.0
CFs	0.0	0.0	0.0	0.0	0.0	12.6	2.4
Ko	0.0	0.0	0.0	0.0	0.0	0.1	2.3
Unit-cell parameters							
a (Å)	9.803(2)	9.744(1)	9.6912(3)	9.6912(1)	9.671(1)	9.773(1)	9.7476(4)
b (Å)	8.985(2)	8.904(2)	8.8986(3)	8.9134(2)	8.834(2)	8.926(1)	8.9478(4)
c (Å)	5.263(1)	5.273(1)	5.2531(3)	5.2450(1)	5.265(1)	5.269(1)	5.2622(2)
β (°)	105.69(1)	106.14(1)	105.990(3)	105.953(2)	106.17(3)	105.75(1)	106.056(2)
V ($Å^3$)	446.29(1)	439.46(1)	435.49(3)	435.60(2)	432.01(2)	442.38(2)	441.06(3)
Average interatomic distances (Å)							
<*M*1–O>	2.097	2.082	2.058	2.052	2.038	2.085	2.077
<*M*2–O>	2.566	2.502	2.505	2.499	2.490	2.502	2.504
<*T*–O>	1.620	1.629	1.636	1.635	1.642	1.640	1.638

References: [(1)] Bindi *et al*. (2002); [(2)] Bindi *et al*. (2006); [(3)] Bindi *et al*. (2003); [(4)] Harlow (1996).
* KKo component is present in clinopyroxene K18a, which seems to be the only K-bearing endmember in this solid solution.

Structural modifications of KCpx at high pressure

The behaviour of KCpx sample 939-1 (Table 1) with an increase in pressure (up to 9.72 GPa) was studied at room temperature using the diamond anvil cell technique (Bindi *et al*., 2006). The fit to the *P-V* data with the third-order Birch-Murnaghan equation corresponds to V_0 = 435.49(3) Å^3, K_0 = 129(1) GPa, and K_0' = 2.7(3) (Bindi *et al*., 2006). When compared to K_0 of pure diopside (112 GPa), these parameters show that the ^{M2}Ca + ^{M1}Mg $\rightleftharpoons$ ^{M2}K + ^{M1}Al substitution leads to a notable increase in the bulk modulus. Bindi *et al*. (2006) showed that the *M*2 polyhedron in the sample 939-1 is much less compressible than the *M*1 polyhedron. These data indicate that the incorporation of K into the clinopyroxene structure has little effect on its compressibility, which is determined primarily by the compressibility of the *M*1 octahedron occupied by Al. Comparison with other clinopyroxenes shows that the *M*1 polyhedron of the 939-1 clinopyroxene is more compressible than FeO_6, AlO_6 and CrO_6 octahedra, but less compressible than MgO_6. Thus, the high compressibility of the *M*1 octahedron seems to be a basic crystal-chemical factor which stabilizes KJd in KCpx solid-solution with pressure by adjusting its size to smaller multi-charged cations (Al).

Thermodynamic modelling of the KCpx solid-solution

The experimental and crystal-chemical data discussed above provide certain constraints on the character of the KCpx solid-solution. Previously, we proposed a semi-empirical thermodynamic model to describe the equilibria of KCpx with melt (Perchuk *et al*., 2002; Safonov *et al*., 2005*b*). However, this model does not include any standard thermodynamic properties for KJd, and thus its application is rather limited. In order to estimate the necessary thermodynamic properties of KJd and its solid solution with diopside, Vinograd *et al*. (2010) performed a computer simulation on the basis of empirical interatomic potentials and *ab initio* calculations. In the present paper, we will use the above experimental and crystal-chemical data as tools for checking predictions based on atomistic calculations, as well as extend the petrologic application of the thermodynamic data obtained in Vinograd *et al*. (2010).

Standard thermodynamic properties of K-jadeite

Vinograd *et al*. (2010) performed density-functional calculations to estimate the standard enthalpy of formation ($\Delta_f H^0$ = −2932.7 kJ/mol), volume (V^0 = 6.479 J mol^{-1} bar^{-1}), and bulk modulus (K_0 = 145 GPa) for K-jadeite (Table 2). The standard entropy (S^0 = 141.24 J mol^{-1} K^{-1}) and thermal-expansion coefficient (α = 3.3×10^{-5} K^{-1}) were predicted from the lattice-dynamic simulations using an empirical force-field model (Table 2). The predicted large bulk modulus of K-jadeite is qualitatively consistent with the value 129 GPa measured for sample 939-1 containing 12 mol.% K-jadeite (Bindi *et al*., 2006; Table 1). The large bulk modulus of K-jadeite is consistent with the smaller molar volume of this pyroxene in comparison to diopside (i.e. 6.619 J mol^{-1} bar^{-1}; Holland and Powell, 1998). The measurements of Bindi *et al.* (2006) show that the unit-cell volumes of clinopyroxene samples 939-1 (435.49 Å^3; Table 1), 939-2 (10 mol.% KJd, 435.6 Å^3) and 927-1 (3.7 mol.% KJd, 438.2 Å^3) (Table 1) are lower than the unit-cell volume of pure diopside (i.e. 439.28 Å^3) and thus confirm the prediction based on atomistic calculations. On the other hand, Bindi *et al.* (2002) showed that the volumes

TABLE 2. Comparison of the estimated thermodynamic properties of K-jadeite $KAlSi_2O_6$ (Vinograd *et al*., 2010) with those of diopside and jadeite (Holland and Powell, 1998).

Endmember	$\Delta_f H$ (kJ mol^{-1})	S (J K^{-1} mol^{-1})	V (J br^{-1} mol^{-1})	K (GPa)	α 10^{-5} (K^{-1})
$KAlSi_2O_6$ (KJd)	−2932.7	141.24	6.479	145	3.3 (298−1298 K)
$CaMgSi_2O_6$ (Di)	−3202.54	142.7	6.619	112	3.3
$NaAlSi_2O_6$ (Jd)	−3027.83	133.5	6.040	128	2.47

of K1 and K2 pyroxenes are larger than that of diopside, and this warrants further investigation.

Mixing properties of the diopside-K-jadeite solid-solution

Vinograd *et al*. (2010) did atomistic simulations of the thermodynamic mixing properties of the diopside–K-jadeite solid-solution using a series of steps. The first step consisted of calculation of the lattice energies of 800 structures within the pyroxene supercell $2 \times 2 \times 4$ (symmetry *C*2/*c*) with composition along the $CaMgSi_2O_6$–$KAlSi_2O_6$ join with varying degrees of order of K/Ca and Mg/Al, using a self-consistent set of empirical interatomic potentials for the system K–Na–Ca–Mg–Al–Si–O. Then the excess static energies of these structures were cluster expanded in a basis set of 37 pair-interaction parameters. These parameters were subsequently used to constrain Monte Carlo simulations of temperature-dependent enthalpies of mixing in the range 273−2023 K. Finally, the free energies of mixing were obtained from the simulation results with thermodynamic integration and used to construct a *T*-*X* phase diagram for the subsolidus of the $CaMgSi_2O_6$–$KAlSi_2O_6$ join at standard pressure (Fig. 6). The simulations predicted complete mixing within the disordered *C*2/*c* phase above 900 K (phase D in Fig. 6). The excess free energies of the disordered phase D were fitted with the polynomial

$$G_{\text{excess}} = x_{\text{Di}}x_{\text{KJd}}\sum_{n=1}^{3}(A_n + TB_n)(x_{\text{KJd}} - x_{\text{Di}})^{2n-2} + H_0 \quad (6)$$

where $H_0 = x_{\text{Di}}x_{\text{KJd}}(x_{\text{Di}}W_1 + x_{\text{KJd}}W_2)$, x_{Di} and x_{KJd} are mole fractions of diopside and K-jadeite, respectively and where $W_1 = -1139.3$ and $W_2 = 129.4$ J/mol (Vinograd *et al*., 2010). The values of the A_n and B_n coefficients for the temperature interval 800−1600ºC estimated by Vinograd *et al*. (2010) are given in Table 3.

At lower temperature, a polynomial fit (6) was not possible because the model predicted stabilization of several intermediate ordered omphacite-like compounds (Fig. 6). The compound C_1 with the composition $Ca_2Mg_2KAlSi_6O_{18}$ (i.e. ⅔diopside and ⅓K-jadeite) has the space group *B*2/*n*. The compound B_1 containing ⁷⁄₁₂diopside and ⁵⁄₁₂K-jadeite is predicted to have the symmetry *P*2/*c* with unit-cell parameters $a = 31.750$ Å, $b = 26.587$ Å, $c = 28.850$ Å, $\beta = 74.156$º. The crystal

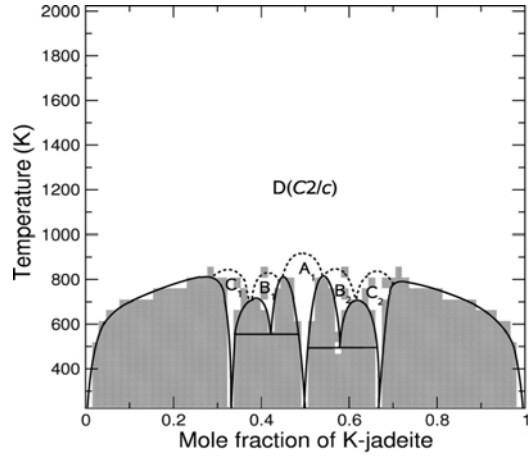

FIG. 6. The *T*-*X* phase diagram for the diopside–K-jadeite solid-solution ($CaMgSi_2O_6$–$KAlSi_2O_6$) constructed from the results of Monte Carlo simulations (Vinograd *et al*., 2010). Dashed lines show an approximate location of the order-disorder transitions to the intermediate ordered phases (see text).

structures of the compounds B_2 and C_2 are similar to those of the compounds B_1 and C_1, and can be obtained from them by substitution of Ca for K and Mg for Al. The most interesting compound in the predicted *T*-*X* diagram (Fig. 6) is the phase A at $X_{\text{KJd}} = 0.5$ (hereafter referred to as K-omphacite). It has *P*2/*n* symmetry and it is analogous to omphacite on the join $CaMgSi_2O_6$–$NaAlSi_2O_6$. However, it has a reverse distribution of monovalent and divalent cations between the M21 and M22 positions, i.e. K and Ca in the K-omphacites are situated at positions which would be occupied by Ca and Na, respectively, in Na-omphacite. According to the density functional calculations of Vinograd *et al*. (2010), K tends to substitute for Ca rather than for Na. The formation of the Mg-K nearest pairs in

TABLE 3. The values of the A_n and B_n coefficients in the polynomial (6) for the temperature interval 800−1600ºC (Vinograd *et al*., 2010).

N	A_n (J mol^{-1})	B_n (J K^{-1} mol^{-1})
1	−2074.4	3.775
2	10879.7	−2.896
3	−662.6	1.468

K-Na-Ca-clinopyroxene costs less energy than the formation of Mg-Na pairs (Vinograd *et al*., 2010). This computational result is in full agreement with the positive correlation of ^{M2}K and ^{M1}Mg in synthetic clinopyroxene of the system $CaMgSi_2O_6$–$NaAlSi_2O_6$–$KAlSi_2O_6$ (Fig. 4*b*) and with the negative effect of jadeite on the solubility of $KAlSi_2O_6$ in clinopyroxene (Safonov *et al*., 2004).

Due to the smaller compressibility of K-jadeite, the difference between the volumes of K-jadeite and diopside decreases significantly with pressure (Fig. 7). As the elastic component of the enthalpy of mixing is proportional to the square of the volume difference between the end members (e.g. Vinograd, 2002), this result implies that the mixing properties of the Di-KJd solid-solution should become closer to ideal as the pressure increases.

Reactions with K-bearing clinopyroxene and their petrological applications

The experimental data on limits of solubility of K-bearing endmembers in clinopyroxene solid-solution, the available X-ray data, and the results of atomistic simulation suggest that small amounts of K in clinopyroxene cannot be caused by a strong non-ideality in the KCpx solid-solution. This is more likely to be the result of specific thermodynamic properties of the K-jadeite endmember, namely, its high molar enthalpy of formation (Table 2). To illustrate this conclusion, we previously (Vinograd *et al*., 2010) calculated KJd contents for clinopyroxenes in the system $CaMgSi_2O_6$–$KAlSi_3O_8$–SiO_2 at pressures above 5 GPa (Fig. 8*a*) using standard thermodynamic properties and thermodynamic mixing parameters derived by Vinograd *et al*. (2010). The KCpx composition in this system is controlled by the equilibrium

$$KJd\ (in\ KCpx) + SiO_2 \rightleftharpoons KAlSi_3O_8 \qquad (7)$$

where SiO_2 is coesite or stishovite, whereas $KAlSi_3O_8$ is sanidine or has the hollandite structure. The relevant thermodynamic parameters of these reactions are given in Table 4. For the reaction with sanidine and coesite, the large negative enthalpy (−126.7 kJ/mol) and the positive entropy (47.96 J mol^{-1} K^{-1}) and volume (2.375 J mol^{-1} bar^{-1}) (Table 4) imply that KJd content in KCpx equilibrated should be very low. However, an increase in the pressure would stabilize KJd in KCpx solid-solution, and thus the mole fraction of K-jadeite in clinopyroxene should increase with increasing pressure (Fig. 8*a*). For the assemblage containing K-feldspar with a hollandite-type structure and stishovite, the opposite tendency is observed (Fig. 8*a*). The change of the slopes of the isopleths in the hollandite and sanidine field is consistent with the signs of volume and entropy effects of the reaction KJd + Sti → Hol. Thus the calculations predict the reverse in the KJd content in clinopyroxene with increasing pressure. A similar reversal was observed by Wang and Takahashi (1999) in subsolidus experiments on natural basalt JB1 over the pressure interval up to 15 GPa. Their experiments show that in the pressure range up to 6 GPa, where the temperature changes along the average mantle geotherm, the K_2O content in clinopyroxene in the assemblage with San + Coe + Grt increases with pressure. At the same time, at pressures above 10 GPa up to the disappearance of clinopyroxene in the presence of K-feldspar with a hollandite-type structure and stishovite, the K_2O content in clinopyroxene decreases with pressure. The maximum K_2O content in clinopyroxene was reached at 7−9 GPa. Similarly, Fig. 8*a* shows that the maximum KJd mole-fraction in clinopyroxene (about 0.11−0.12) is reached within the same pressure range along the mantle geotherm. On the other hand, the thermodynamic calculations predict that the mole fraction of K-jadeite increases with temperature in both assemblages (Fig. 8*a*). Similar behaviour was observed in the subsolidus experiments of Schmidt and Poli (1998) at 10 GPa.

Here we should note that the agreement discussed above between the calculations and

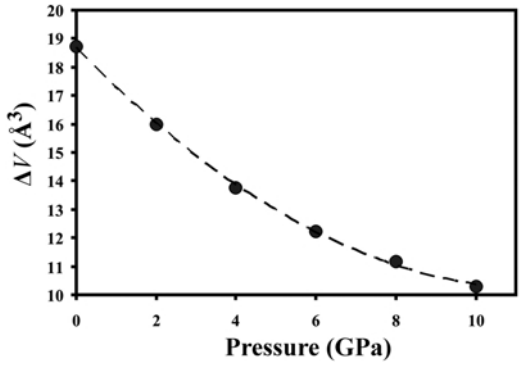

FIG. 7. The estimated volume mismatch between diopside and K-jadeite as a function of pressure (Vinograd *et al*., 2010).

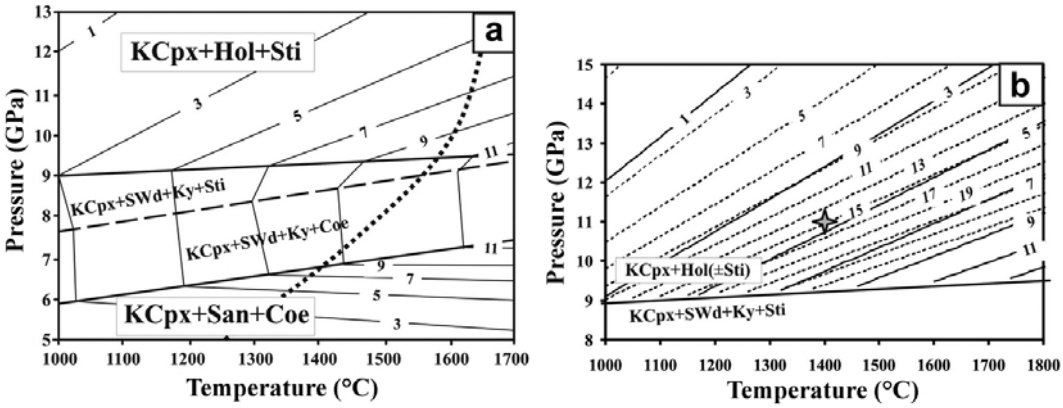

FIG. 8. Lines of constant mol.% of KJd in clinopyroxene and the reaction boundaries in assemblages in the system $CaMgSi_2O_6$–$KAlSi_3O_8$–SiO_2 as functions of *P* and *T*. (*a*) Lines of constant mole percent of KJd in clinopyroxene (thin solid lines with numbers) and the reaction boundaries (thick or dashed lines) in the assemblages containing free SiO_2 (coesite or stishovite). The figure is slightly modified after Vinograd *et al*. (2010). (*b*) Comparison of lines of constant mole percent of KJd in clinopyroxene in the assemblage Cpx + Hol + Sti (see Fig. 8*a*) (solid lines with straight labels) and in the assemblage Cpx + Hol undersaturated with silica (for $a_{SiO_2} = 0.2$) (dashed lines with italic labels). The grey star denotes *P-T* conditions of Harlow's (1999) experiment TT155, where clinopyroxene with 15−17 mol.% of KJd has been produced. Thermodynamic parameters for KJd and diopside–KJd solid-solution are taken from Vinograd *et al*. (2010) based on the following data: coesite, kyanite, sanidine, stishovite from Holland and Powell (1998); Si-wadeite and K-feldspar with a hollandite structure from Yong *et al*. (2006). The method of calculation was described by Vinograd *et al*. (2010). Thick dotted line denotes an average mantle geotherm (Akaogi *et al*., 1989).

the experiments should be judged as qualitative. The computed isopleths (Fig. 8*a*) correspond to the Na-free system, whereas compositions of synthetic clinopyroxenes are more complicated. The presence of garnet and high-jadeite clinopyroxene is not taken into account in the present calculations, nor is the presence of the Ca-Eskola component, which is a common feature of high-pressure clinopyroxenes (e.g. Konzett *et al*., 2008). For example, the experiments of Schmidt and Poli (1998) show ~1 wt.% K_2O, i.e. 4−5 mol.% of KJd, in clinopyroxene at 1000ºC and 10 GPa. Figure 8*a* predicts about 2.5 mol.% KJd at these conditions. The mole fractions of 15−17 mol.% of KJd in clinopyroxene measured by Harlow (1999) in association with K-feldspar with a hollandite-type structure at 11 GPa and 1400ºC are much higher than those obtained in the calculations. Figure 8*a* predicts about 5 mol.% KJd at these conditions. However, such a large difference cannot be attributed to inaccuracy of the derived thermodynamic constants. The discrepancy could also be due to the absence of free silica (stishovite) in the products of Harlow's (1999) runs. In order to test this possibility, we recalculated isopleths of X_{KJd} in clinopyroxene for the equilibrium r2 (Table 4) at SiO_2 activity (standardized to stishovite) lower than 1.0 (Fig. 8*b*). Our calculations show that the absence of free SiO_2 leads to stabilization of clinopyroxene with much higher content of KJd. At $a_{SiO_2} = 0.2$, the data point of Harlow's (1999) experiment (15 mol.% KJd at 11 GPa and 1400ºC) is in good agreement with the calculated isopleths (Fig. 8*b*). It thus seems that free silica destabilizes the KJd component in clinopyroxene solid-solution. Similar conclusions were expressed earlier in a study of the system $CaMgSi_2O_6$-$KAlSi_3O_8$ at 6 GPa (Safonov *et al*., 2005*a*) and in a study of natural K-bearing clinopyroxenes (Perchuk *et al*., 2002).

Mineral assemblages containing $KAlSi_3O_8$ polymorphs are typical of high-pressure metamorphosed pelites and rocks of eclogitic composition. In fact, the compositional features of most natural KCpx suggest an eclogite-like source, whereas examples of peridotitic K-rich clinopyroxenes are relatively scarce (Daniels and Gurney, 1989; Jaques *et al*., 1990; Harlow and Veblen, 1991; Harlow, 1996). Interestingly, no K-rich clinopyr-

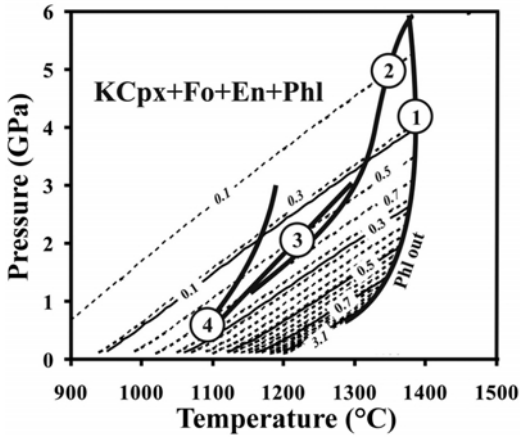

FIG. 9. Lines of constant mol.% of KJd in clinopyroxene for equilibrium KJd (in KCpx) + 2Fo + H_2O = En + Phl (r3 in Table 4) as functions of P and T for a_{H_2O} = 1.0 (solid thin lines with straight labels) and a_{H_2O} = 0.1 (dashed thin lines with italic labels). Thick lines: (1) phlogopite stability curve (Trønnes, 2002); (2) and (3) solidus curves for the water-undersaturated system Phl + Di from Luth (1997) and Modreski and Boettcher (1973); (4) solidus curve for the water-oversaturated system Phl + Di + H_2O (Modreski and Boettcher, 1973). Thermodynamic parameters for KJd and diopside-KJd solid-solution are taken from Vinograd *et al*. (2010) for enstatite, forsterite, phlogopite and water vapour data are from Holland and Powell (1998).

oxenes were documented in association with phlogopite. In order to characterize the behaviour of the KJd content in clinopyroxene in the peridotite assemblage Ol + Opx + Cpx + Phl, we have calculated KJd contents in clinopyroxenes for the equilibrium KJd + 2Fo + $H_2O \rightleftharpoons$ En + Phl (Fig. 9; Table 4). Compared to the $KAlSi_3O_8$-bearing equilibria, this reaction shows a much higher negative enthalpy effect, suggesting that phlogopite is a much stronger competitor for K compared to sanidine. Figure 9 shows that clinopyroxene associated with forsterite, enstatite and phlogopite contains much lower concentrations of the KJd endmember in comparison to clinopyroxenes associated with $KAlSi_3O_8$ polymorphs (Fig. 8*a*,*b*). Within the phlogopite stability field, at unit activity of water, clinopyroxene contains less than 1 mol.% KJd. At the same time, low water activity strongly assists the accumulation of K in clinopyroxene. Another specific feature of KCpx equilibria in association with phlogopite is the positive slope of the KJd isopleths (Fig. 9), which indicates that the KJd content in clinopyroxene decreases with pressure and increases with temperature. Indeed, Luth (1997) reported an increase of the KJd content in clinopyroxene from 0.6 mol.% to 1.5 mol.% in the assemblage with Phl and Fo with increase in temperature from 1200 to 1350ºC at 5 GPa. However, Luth (1997) noted that in the diopside-phlogopite system, the KJd content in clinopyroxene increases with pressure. This inconsistency with the calculations can be attributed to the change of mineral assemblage with pressure in Luth's (1997) experiments: the leap of the KJd content in clinopyroxene from 0.9 mol.% at 5 GPa to 3.6 mol.% at 7.5 GPa coincides with the appearance of garnet. The presence of Ca-bearing garnet is not taken into account in Fig. 9. The experiments of Luth (1997) were done at vapour-free conditions, i.e. at $a_{H_2O} << 1.0$. We are not aware of similar experiments at high pressure in the presence of free water. Modreski and Boettcher (1973) studied the phlogopite-diopside system at pressures up to 3.0 GPa at

TABLE 4. Estimated thermodynamic effects of some petrologically useful mineral reactions involving KJd discussed in the text.

Reaction number	Reaction	$\Delta H_{298,\ 1}$ (kJ mol^{-1})	$\Delta S_{298,\ 1}$ (J K^{-1} mol^{-1})	$\Delta V_{298,\ 1}$ (J br^{-1} mol^{-1})
r1	KJd + Coe → San	−126.68	47.96	2.375
r2	KJd + Sti → Hol	4.88	0.46	−0.752
r3	KJd + 2Fo + H_2O → En + Phl	−246.36	−125.99	2.884
r4	KJd + Coe → $KAlSi_3O_8$ (liquid)	−133.66	−39.04	2.856

Thermodynamic parameters for KJd were derived in Vinograd *et al*. (2010). Thermodynamic data on coesite, kyanite, sanidine, phlogopite, enstatite, forsterite and water vapour are from Holland and Powell (1998), while those on Si-wadeite and $KAlSi_3O_8$–hollandite are from Yong *et al*. (2006).

water-undersaturated and water-oversaturated conditions. Their data show that the KJd content in clinopyroxene produced in mixtures Phl + Di and Phl + Di + En without excess water at 1.0–2.0 GPa and 1150–1250ºC varies from 0.5 to 0.8 mol.%, while it is 0.1–0.5 mol.% in clinopyroxenes synthesized in the presence of excess water vapour (assuming a_{H_2O} close to 1.0) at the same *P-T* conditions. These data are in good agreement with the calculated isopleths. Further, Fig. 9 suggests that clinopyroxene with up to 2–3 mol.% of the K-jadeite endmember could be stable in the presence of phlogopite at relatively low pressure (1.0–2.0 GPa) and temperature (1200–1350ºC) where water activity remains low. These are exactly the *P-T*-fluid conditions for the generation of some K-rich magmas from a peridotitic source (e.g. Foley, 1992). Such increase of K-content in clinopyroxene coexisting with phlogopite at relatively high temperature and low pressure could explain K-enrichment of clinopyroxene megacrysts found in K-rich magmatic rocks of the upper-mantle origin (Ghorbani and Middlemost, 2000; Plá Cid *et al*., 2003).

Many authors (e.g. Luth, 1997; Mitchell, 1995; Schmidt and Poli, 1998; Tsuruta and Takahashi, 1998; Okamoto and Maruyama, 1998; Wang and Takahashi, 1999) have pointed out that, although the K-content of clinopyroxene increases with temperature at subsolidus conditions, it drops abruptly in the presence of melt. Our experiments in the $CaMgSi_2O_6$–$KAlSi_2O_6$ and $CaMgSi_2O_6$–$KAlSi_3O_8$ systems at 7 and 6 GPa (Safonov *et al*., 2003, 2005*a*) unambiguously show a continuous decrease of the KJd content above the solidus. However, increase of the KJd mole-fraction with pressure remains valid even in the presence of a melt. Thus, the isopleths of KJd content in equilibrium with a K-rich melt should have positive slope. This is indeed the case (Fig. 10) for the equilibrium KJd (in Cpx) + Coe = $KAlSi_3O_8$-liquid (r4 in Table 4). As seen in Fig. 10, the decrease in the activity of the $KAlSi_3O_8$ component in the melt results in a shift of the isopleths to higher pressure. This prediction is consistent with the results of many experimental studies (Edgar and Vukadinovic, 1993; Mitchell, 1995; Edgar and Mitchell, 1997; Harlow, 1999; Safonov *et al*., 2003, 2004, 2005*b*) showing that K-rich clinopyroxene can be crystallized at lower pressure in the presence of K-rich silicate melt. Thus K-bearing clinopyroxene is an indicator of the presence of such liquids in the upper mantle.

Conclusions

The estimated thermodynamic standard properties of the K-jadeite endmember and the parameters of mixing of the solid solution of diopside-K-jadeite are in good agreement with the major tendencies in the variation of K-content in clinopyroxenes in a wide *P-T* interval in diverse phase assemblages. The calculated compositions of KCpx are in good qualitative agreement with the available experimental data. Both the experiments and the thermodynamic calculations show that at pressures of ~5 GPa (120–150 km of depth), clinopyroxene is able to accommodate up to 1.0 wt.% K_2O. Taking into account a large modal content of clinopyroxene in upper-mantle rocks, KCpx can surely serve a host of K that is responsible both for the radioactive heat and for the highly potassic fluids acting throughout the upper mantle and lower crust.

Acknowledgements

This paper is dedicated to the late Prof. Leonid L. Perchuk, whose ideas created a basis for the present study. The manuscript benefited from the reviews of Robert Luth, George Harlow and

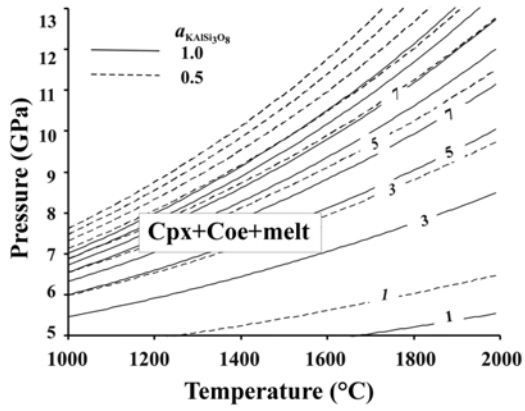

FIG. 10. Lines of constant mol.% of KJd in clinopyroxene in the assemblage with coesite and K-rich aluminosilicate melt in the system $CaMgSi_2O_6$–$KAlSi_3O_8$–SiO_2 as functions of *P* and *T* at different activities of $KAlSi_3O_8$ in the melt, $a_{KAlSi_3O_8} = 1.0$ (solid lines with straight numbers) and $a_{KAlSi_3O_8} = 0.5$ (dashed lines with italic numbers). The method of calculation was described by Vinograd *et al*. (2010). Thermodynamic data on coesite and $KAlSi_3O_8$ melt are taken from Holland and Powell (1998).

Frank Hawthorne. The study is supported by the Russian Foundation for Basic Research (project 10-05-00040) and the RF President's Grants MD-380.2010.5 (to OGS). VLV acknowledges the support of the Helmholtz Society (The Virtual Institute for the Advanced Solid and Aqueous Radiogeochemistry).

References

Akaogi, M., Ito, E. and Navrotsky, A. (1989) Olivine-modified spinel transition in the system Mg_2SiO_4-Fe_2SiO_4: calorimetric measurements, thermochemical calculation, and geophysical application. *Journal of Geophysical Research*, **94**, 15671–15685.

Arima, M. and Onuma, K. (1977) The solubility of alumina in enstatite and the phase equilibria in the join $MgSiO_3$-$MgAl_2SiO_6$ at 10–25 kbar. *Contributions to Mineralogy and Petrology*, **61**, 251–265.

Benna, P., Chiari, G. and Bruno, E. (1987) Structural modifications in clinopyroxene solid solution: the Ca-Mg and Ca-Sr substitutions in the diopside structure. *Mineralogy and Petrology*, **36**, 71–84.

Bindi, L., Safonov, O.G., Litvin, Yu.A., Perchuk, L.L. and Menchetti, S. (2002) Ultrahigh potassium content in the clinopyroxene structure: an X-ray single-crystal study. *European Journal of Mineralogy*, **14**, 929–934.

Bindi, L., Safonov, O.G., Yapaskurt, V.O., Perchuk, L.L. and Menchetti, S. (2003) Ultrapotassic clinopyroxene from the Kumdy-Kol microdiamond mine, Kokchetav Complex, Kazakhstan: occurrence, composition and crystal-chemical characterization. *American Mineralogist*, **88**, 464–468.

Bindi, L., Downs, R.T., Harlow, G.E., Safonov, O.G., Litvin, Yu.A., Perchuk, L.L. and Menchetti, S. (2006) Compressibility of synthetic potassium-rich clinopyroxene: In-situ high-pressure single-crystal X-ray study. *American Mineralogist*, **91**, 802–808.

Bishop, F.C., Smith, J.V. and Dawson, J.B. (1978) Na, K, P and Ti in garnet, pyroxene and olivine from peridotite and eclogite xenoliths from African kimberlites. *Lithos*, **11**, 155–173.

Carpenter, M.A. (1980) Mechanisms of exsolution in sodic pyroxenes. *Contributions to Mineralogy and Petrology*, **71**, 289–300.

Chudinovskikh, L.T., Zharikov, V.A., Ishbulatov, R.A. and Matveev, Y.A. (2001) On the mechanism of incorporation of ultra-high amounts of potassium into clinopyroxene at high pressure. *Doklady Earth Sciences*, **380**, 1–4.

Daniels, L.R.M. and Gurney, J.J. (1989) The chemistry of garnets, chromites and diamond inclusions from the Dokolwayo kimberlites, Kingdom of Swaziland. Pp. 1012–1021 in: *Kimberlites and related rocks. Volume 2. Their Mantle/Crust Setting, Diamonds and Diamond Exploration* (J. Ross, editor). Geological Society of Australia Special Publication, **14**. Blackwell, Carlton, Australia.

Edgar, A.D. and Mitchell, R.H. (1997) Ultra high pressure-temperature melting experiments on an SiO_2-rich lamproite from Smoky Butte, Montana: derivation of siliceous lamproite magmas from enriched sources deep in the continental mantle. *Journal of Petrology*, **38**, 457–477.

Edgar, A.D. and Vukadinovic, D. (1993) Potassium-rich clinopyroxene in the mantle: an experimental investigation of K-rich lamproite up to 60 kbar. *Geochimica et Cosmochimica Acta*, **57**, 5063–5072.

Erlank, A.J. and Kushiro, I. (1970) Potassium contents of synthetic pyroxenes at high temperatures and pressures. *Carnegie Institution Washington Yearbook*, **68**, 267–271.

Foley, S.F. (1992) Petrological characterization of the source components of potassic magmas: geochemical and experimental constraints. *Lithos*, **28**, 187–204.

Foley, S.F., Yaxley, G.M., Rosenthal, A., Buhre, S., Kiseeva, E.S., Rapp, R.P. and Jacob, D.E. (2009) The composition of near-solidus melts of peridotite in the presence of CO_2 and H_2O between 40 and 60 kbar. *Lithos*, **112S**, 274–283.

Ghorbani, M.R. and Middlemost, E.A.K. (2000) Geochemistry of pyroxene inclusions from the Warrumbungle Volcano, New South Wales, Australia. *American Mineralogist*, **85**, 1349–1367.

Harlow, G.E. (1996) Structure refinement of natural K-rich diopside: the effect of K on the average structure. *American Mineralogist*, **81**, 632–638.

Harlow, G.E. (1997) K in clinopyroxene at high pressure and temperature: an experimental study. *American Mineralogist*, **82**, 259–269.

Harlow, G.E. (1999) Interpretation of Kcpx and CaEs in Clinopyroxene from Diamond Inclusions and Mantle Samples. Pp. 321–331 in: *Proceedings of Seventh International Kimberlite Convention*, *volume I* (J.J. Gurney, J.L. Gurney, M.D. Pascoe and S.H. Richardson, editors). Redroof Design, Cape Town, South Africa.

Harlow, G.E. (2002) Diopside + F-rich phlogopite at high P and T: Systematics, crystal chemistry and stability of $KMgF_3$, clinohumite and chondrodite. *Geological Materials Research*, **4**, 1–28.

Harlow, G.E. and Davies, R. (2004) Status report on stability of K-rich phases at mantle conditions. *Lithos*, **77**, 647–653.

Harlow, G.E. and Veblen, D.R. (1991) Potassium in clinopyroxene inclusions from diamonds. *Science*, **251**, 652–655.

Hart, S. R. and Zindler, A. (1986) In search of a bulk-earth composition. *Chemical Geology*, **57**, 247–267.

Holland, T.J.B. and Powell, R. (1998) An internally-consistent thermodynamic data set for phases of petrological interest. *Journal of Metamorphic Geology*, **16**, 309–343.

Ikeda, K. and Yagi, K. (1972) Synthesis of kosmochlor and phase equilibria in the join $CaMgSi_2O_6$-$NaCrSi_2O_6$. *Contributions to Mineralogy and Petrology*, **36**, 63–72.

Jagoutz, E., Palme, H., Baddenhausen, H., Blum, K., Cendales, M., Dreibus, G., Spettel, B., Lorenz, V. and Wänke H. (1979) The abundances of major, minor and trace elements in the Earth's mantle as derived from primitive ultramafic nodules. Pp. 2031–2050 in: *Proceedings of the 10th Lunar and Planetary Science Conference*, (R.B. Merrill editor). Geochimica et Cosmochimica Acta Supplement **11**. Pergamon Press, New York.

Jaques, A.L., O'Neill, H.St.C, Smith, C.B., Moon, J. and Chappell, B.W. (1990) Diamondiferous peridotite xenoliths from the Argyle (AK1) lamproite pipe, Western Australia. *Contributions to Mineralogy and Petrology*, **104**, 255–276.

Kaminsky, F.V., Zakharchenko, O.D., Griffin, W.L., Channer, DeR. D. M. and Khachatryan-Blinova, G.K. (2000) Diamond from the Guaniamo area, Venezuela. *The Canadian Mineralogist*, **38**, 1347–1370.

Konzett, J. and Fei, Y. (2000) Transport and storage of potassium in the Earth's upper mantle and transition zone: experimental study to 23 GPa in simplified and natural bulk compositions. *Journal of Petrology*, **41**, 583–603.

Konzett, J. and Ulmer, P. (1999) The stability of hydrous potassic phases in lherzolitic mantle – an experimental study to 9.5 GPa in simplified and natural bulk compositions. *Journal of Petrology*, **40**, 629–652.

Konzett, J., Frost, D.J., Proyer, A. and Ulmer, P. (2008) The Ca-Eskola component in eclogitic clinopyroxene as a function of pressure, temperature and bulk composition: an experimental study to 15 GPa with possible implications for the formation of oriented SiO_2-inclusions in omphacite. *Contributions to Mineralogy and Petrology*, **155**, 215–228.

Liu, L. (1987) High-pressure transition of potassium aluminosilicates with an emphasis on leucite. *Contributions to Mineralogy and Petrology*, **95**, 1–3.

Luth, R.W. (1992) Potassium in clinopyroxene at high pressure: experimental constraints. *EOS Transactions of the American Geophysical Union*, **73**, 608.

Luth, R.W. (1995) Potassium in clinopyroxene at high pressure. *EOS Transactions of the American Geophysical Union*, **76**, F711.

Luth, R.W. (1997) Experimental study of the system phlogopite-diopside from 3.5 to 17 GPa. *American Mineralogist*, **82**, 1198–1209.

Matveev, Yu.A., Chudinovskikh, L.T. and Litvin, Yu.A. (2000) Formation of potassium-rich clinopyroxenes and carbonate-silicate melting relations in the $K_2(Ca,Mg)(CO_3)_2$-clinopyroxene-garnet system at 3.8–7.0 GPa: Modeling the genesis of diamond-bearing rocks of Kazakhstan metamorphic complex. *Journal of Conference Abstracts VIII Symposium EMPG*, Bergamo, **5** (1).

McDonough, W. F. and Sun, S.-S. (1995) The composition of the Earth. *Chemical Geology*, **120**, 223–253.

McDonough, W.F., Sun, S.-S., Ringwood, A.E., Jagoutz, E. and Hofmann, A.W. (1992) Potassium, rubidium, and cesium in the Earth and Moon and the evolution of the mantle of the Earth. *Geochimica et Cosmochimica Acta*, **56**, 1001–1012.

Mellini, M. and Cundari, A. (1989) On the reported presence of potassium in clinopyroxene from potassium-rich lavas: a transmission electron microscope study. *Mineralogical Magazine*, **53**, 311–314.

Mitchell, R.H. (1995) Melting experiments on a sanidine-phlogopite lamproite at 4–7 GPa and their bearing on the source of lamproitic magmas. *Journal of Petrology*, **36**, 1455–1474.

Modreski, P.J. and Boettcher, A.L. (1973) Phase relationships of phlogopite in the system K_2O-MgO-CaO-Al_2O_3-SiO_2-H_2O to 35 kbars: a better model for mica in the interior of the Earth. *American Journal of Sciences*, **273**, 385–414.

Newton, R.C., Charlu, T.V. and Kleppa, O.J. (1977) Thermochemistry of high pressure garnets and clinopyroxenes in the system CaO-MgO-Al_2O_3-SiO_2. *Geochimica et Cosmochimica Acta*, **41**, 369–377.

Okamoto, K. and Maruyama, S. (1998) Multi-anvil re-equilibration experiments of a Dabie Shan ultra-high pressure eclogite within the diamond-stability fields. *Island Arc*, **7**, 52–69.

Okamura, F.P., Ghose, S. and Ohashi, H. (1974) Structure and crystal chemistry of calcium Tschermack's pyroxene, $CaAlAlSiO_6$. *American Mineralogist*, **59**, 549–557.

Papike, J.J. (1980) Pyroxene mineralogy of the Moon and meteorites. Pp 495–525 in: *Pyroxenes* (C.T. Prewitt, editor). Reviews in Mineralogy and Geochemistry, **7**, Mineralogical Society of America, Washington D.C.

Perchuk, L.L., Safonov, O.G., Yapaskurt, V.O. and Barton, J.M., Jr. (2002) Crystal-melt equilibria involving potassium-bearing clinopyroxene as indicators of mantle-derived ultrahigh-potassic liquids: an analytical review. *Lithos*, **60**, 89–111.

Plá Cid, J., Nardi, L.V.S., Stabel, L.Z., Conceição, R.V.

and Balzaretti, N.M. (2003) High-pressure minerals in mafic microgranular enclaves: evidences for co-mingling between lamprophyric and syenitic magmas at mantle conditions. *Contributions to Mineralogy and Petrology*, **145**, 444–459.

Pokhilenko, N.P., Sobolev, N.V., Reutsky, V.N., Hall, A.E. and Taylor, L.A. (2004) Crystalline inclusions and C-isotope ratios in diamonds from the Snap Lake/King Lake kimberlite dyke system: evidence of ultradeep and enriched lithospheric mantle. *Lithos*, **77**, 57–67

Prinz, M., Manson, D.V., Hlava, P.F. and Keil, K. (1975) Inclusions in diamonds: garnet lherzolite and eclogite assemblages. *Physics and Chemistry of the Earth*, **9**, 797–815.

Ricard, R.S., Harris, J.W., Gurney, J.J. and Cardoso, P. (1989) Mineral inclusions in diamonds from the Koffiefontein Mine. *Geological Society of Australia Special Publications*, **14**, 1054–1062.

Safonov, O.G., Matveev, Y.A., Litvin, Y.A. and Perchuk, L.L. (2002) Experimental study of some joins of the system $CaMgSi_2O_6$-$(Ca,Mg)_3Al_2Si_3O_{12}$-$KAlSi_2O_6$-$K_2(Ca,Mg)(CO_3)_2$ at 5–7 GPa in relation to the genesis of garnet-clinopyroxene-carbonate rocks of the Kokchetav Complex (northern Kazakhstan). *Petrology*, **10**, 519–539.

Safonov, O.G., Litvin, Yu.A., Perchuk, L.L., Bindi, L. and Menchetti, L. (2003) Phase relations of potassium-bearing clinopyroxene in the system $CaMgSi_2O_6$-$KAlSi_2O_6$ at 7 GPa. *Contributions to Mineralogy and Petrology*, **146**, 120–133.

Safonov, O.G., Litvin, Y.A. and Perchuk, L.L. (2004) Synthesis of omphacites and isomorphic features of clinopyroxenes in the system $CaMgSi_2O_6$-$NaAlSi_2O_6$-$KAlSi_2O_6$. *Petrology*, **12**, 84–97.

Safonov, O.G., Perchuk, L.L., Litvin, Yu.A. and Bindi, L. (2005*a*) Phase relations in the $CaMgSi_2O_6$-$KAlSi_3O_8$ join at 6 and 3.5 GPa as a model for formation of some potassium-bearing deep-seated mineral assemblages. *Contributions to Mineralogy and Petrology*, **149**, 316–337.

Safonov, O.G., Perchuk, L.L. and Litvin, Yu.A. (2005*b*) Equilibrium K-bearing clinopyroxene-melt as a model for barometry of mantle-derived mineral assemblages. *Russian Geology and Geophysics*, **46**, 1318–1334.

Safonov, O.G., Perchuk, L.L. and Litvin, Yu.A. (2006) Effect of carbonates on crystallization and composition of potassium-bearing clinopyroxene at high pressures. *Doklady Earth Sciences*, **408**, 580–585.

Schmidt, M.W. (1996) Experimental constraints on recycling potassium from subducted oceanic crust. *Science*, **272**, 1927–1930.

Schmidt, M.W. and Poli, S. (1998) Experimentally based water budgets for dehydrating slabs and consequences for arc magma generation. *Earth and Planetary Science Letters*, **163**, 361–379.

Shannon, R.D. (1976) Revised effective ionic radii and systematic studies of interatomic distances in halides and chalcogenides. *Acta Crystallographica*, **A32**, 751–767.

Shimizu, N. (1971) Potassium content of synthetic clinopyroxenes at high pressures and temperatures. *Earth and Planetary Science Letters*, **11**, 374–380.

Sobolev, N. V. (1977) *Deep-seated inclusions in kimberlites and the problem of the composition of the upper mantle*. AGU, Washington, 279 pp. [Translated from the Russian edition, 1974].

Sobolev, N.V. and Shatsky, V.S. (1990) Diamond inclusions in garnets from metamorphic rocks: a new environment for diamond formation. *Nature*, **343**, 742–746.

Sobolev, N.V., Yefimova, E.S., Channer, D. M. DeR., Anderson, P.F.N. and Barron, K.M. (1998) Unusual upper mantle beneath Guaniamo, Guyana Shield, Venezuela: evidence from diamond inclusions. *Geology*, **26**, 971–974.

Spandler, C., Yaxley, G., Green, D. H. and Rosenthal, A. (2008) Phase relations and melting of anhydrous K-bearing eclogite from 1200 to 1600ºC and 3 to 5 GPa. *Journal of Petrology*, **49**, 771.

Stachel, T., Brey, G.P. and Harris, J.W. (2000) Kankan diamonds (Guinea) I: from the lithosphere down to the transition zone. *Contributions to Mineralogy and Petrology*, **140**, 1–15.

Swanson, D.K. and Prewitt, C.T. (1983) The crystal structure of $K_2Si^{VI}Si_3^{IV}O_9$. *American Mineralogist*, **68**, 581–585.

Thomsen, T.B. and Schmidt, M.W. (2008) Melting of carbonated pelites at 2.5–5.0 GPa, silicate–carbonatite liquid immiscibility, and potassium–carbon metasomatism of the mantle. *Earth and Planetary Science Letters*, **267**, 17–31.

Trønnes, R.G. (2002) Stability range and decomposition of potassic richterite and phlogopite end members at 5–15 GPa. *Mineralogy and Petrology*, **74**, 129–148.

Tsuruta, K. and Takahashi, E. (1998) Melting study of an alkali basalt JB-1 up to 12.5 GPa: behavior of potassium in the deep mantle. *Physics of the Earth and Planetary Interiors*, **107**, 119–130.

Vinograd, V.L. (2002) Thermodynamics of mixing and ordering in the diopside¡jadeite system: I. A CVM model. *Mineralogical Magazine*, **66**, 513–536.

Vinograd, V.L., Safonov, O.G., Wilson, D.J., Bindi, L., Gale, J.D., Perchuk, L.L. and Winkler, B. (2010) Thermodynamics of diopside-K-jadeite, $CaMgSi_2O_6$-$KAlSi_2O_6$, solid solution from quantum mechanical and static lattice energy calculations. *Petrology*, **18**, 447–459.

Wang, W. and Takahashi, E. (1999) Subsolidus and melting experiments of a K-rich basaltic composition

to 27 GPa: Implication for behavior of potassium in the mantle. *American Mineralogist*, **84**, 357–361.

Wood, B.J. and Henderson, C.M.B. (1978) Compositions and unit-cell parameters of synthetic non-stoichiometric tschermakitic clinopyroxenes. *American Mineralogist*, **63**, 66–72.

Wood, B.J. and Nichols, J. (1978) The thermodynamic properties of reciprocal solid solutions. *Contributions to Mineralogy and Petrology*, **66**, 389–400.

Wood, B.J., Holland, T.J.B., Newton, R.C. and Kleppa, O.J. (1980) Thermochemistry of jadeite-diopside pyroxenes. *Geochimica et Cosmochimica Acta*, **44**, 1363–1371.

Yong, W., Dachs, E., Withers, A.C. and Essene, E.J. (2006) Heat capacity and phase equilibria of hollandite polymorph of $KAlSi_3O_8$. *Physics and Chemistry of Minerals*, **33**, 167–177.

Appendix

Phases and endmembers:

Ca-Esk: Ca-Eskola pyroxene ($Ca_{0.5}AlSi_2O_6$)
Ca-Ts: Ca-Tschermak pyroxene ($CaAl_2SiO_6$)
CEn: clinoenstatite ($Mg_2Si_2O_6$)
CFs: clinoferrosilite ($Fe_2Si_2O_6$)
Coe: coesite (SiO_2)
Cpx: clinopyroxene
Crd: cordierite ($Mg_2Al_4Si_5O_{18}$)
Di: diopside ($CaMgSi_2O_6$)
En: enstatite ($Mg_2Si_2O_6$)
Fo: forsterite (Mg_2SiO_4)
Grt: garnet
Grs: grossular ($Ca_3Al_2Si_3O_{12}$)
Hed: hedenbergite ($CaFeSi_2O_6$)
Jd: jadeite ($NaAlSi_2O_6$)
Hol: K-feldspar with a hollandite structure ($KAlSi_3O_8$)
KCpx: potassium-bearing clinopyroxene
KJd: potassium jadeite ($KAlSi_2O_6$)
KKo: potassium kosmochlor ($KCrSi_2O_6$)
Ko: kosmochlor ($NaCrSi_2O_6$)
Ks: kalsilite ($KAlSiO_4$)
Ky: kyanite (Al_2SiO_5)
L: melt
Mg-Ts: Mg-Tschermak pyroxene ($MgAl_2SiO_6$)
Opx: orthopyroxene
Phl: phlogopite ($KMg_3AlSi_3O_{10}[OH]_2$)
Prp: pyrope ($Mg_3Al_2Si_3O_{12}$)
San: sanidine ($KAlSi_3O_8$)
Sti: stishovite (SiO_2)
SWd: Si-wadeite ($K_2Si_4O_9$).

Thermodynamic symbols:

P: pressure
T: temperature
N_{KJd}^{Cpx}: molar per cent of KJd in Cpx
a_{SiO_2}: silica activity
a_{H_2O}: water activity.